PHYSICAL REVIEW D VOLUME 50, NUMBER 6 15 SEPTEMBER 1994

Signal-to-noise ratio analysis for a back-action-evading measurement on a double harmonic oscillator

C. Cinquegrana, E. Majorana, N. Pergola, P. Puppo, P. Rapagnani, and F. Ricci
Dipartimento di Fisica, Università di Roma "La Sapienza"
and Istituto Nazionale di Fisica Nucleare, Sezione di Roma, Piazzale Aldo Moro 2–00185, Rome, Italy
(Received 21 January 1994)

We compute the sensitivity of a double harmonic oscillator system inserted in a back-action-evasion scheme of electromechanical transduction. This sensitivity is presented by deriving the effective temperature and the optimum observation time of the detector. Finally, the performances of this scheme on a resonant gravitational wave antenna at low temperature are discussed.

PACS number(s): 04.80.Nn, 06.70.Mx, 43.38.+n

I. INTRODUCTION

To monitor the status of a mechanical harmonic oscillator an electromechanical power conversion must be provided [1]. It has been pointed out that better performances are reached when a resonant transducer, tuned to the oscillator, is used. A typical example of this scheme is given by the gravitational wave (GW) bar detectors currently under development by several groups in the world. In this case the first oscillator is the actual probe of the external impulsive forces and the second oscillator is involved in the power conversion process. The behavior of the whole system is basically that one of a two coupled harmonic oscillators [2] as we discuss in Sec. II.

If a linear scheme is operated, the monitoring sensitivity is limited because of the back-action narrow band noise, due to the electronic amplifier located at the end of the detection apparatus [3]. A nonlinear transduction scheme can be performed by coupling dynamically the double mechanical oscillator, whose angular frequencies are ω_- and ω_+, to an electric oscillator with angular frequency $\omega_e \gg \omega_-, \omega_+$ (Sec. III) [4,5]. In this experimental setup the transducer must be more complex in order to limit the effect due to other noise sources. Then, the coupling of the double mechanical oscillator to the electrical one is obtained by inserting the resonant electromechanical transducer into a parametric bridge (parabridge) [6–8] (Sec. IV). Here we present a theoretical model which deals with all basic requirements which must be satisfied to study and improve the features of the experiment (Sec. V). In Sec. VI the signal-to-noise ratio (SNR) analysis is presented and discussed in the framework of the current generation of GW bar antennas.

II. THE SYSTEM: A MECHANICAL DOUBLE HARMONIC OSCILLATOR

The theoretical and experimental background of this issue is related with the improvement of the sensitivity of the gravitational wave resonant antennas. We usually deal with a system whose features are similar to those of massive cryogenic resonant bar detectors. In the model of two oscillators in series the first harmonic oscillator schematizes the first longitudinal vibration mode of the massive cylinder (bar) and the second one represents the resonant capacitive transducer clamped on one of its faces [1]. The Hamiltonian of the system is

$$H=\frac{p_x^2}{2m_x}+\frac{1}{2}m_x\omega_x^2x^2+\frac{p_y^2}{2m_y}+\tfrac{1}{2}m_x w_x(y-x)^2-f_x x-f_y y\ , \tag{1}$$

where f_x and f_y are the external forces applied to the oscillators. Here we have 2 degrees of freedom and two normal modes of vibration. By defining $\mu=m_y/m_x$ and ν_x, ν_y the frequencies of the uncoupled oscillators, it can be shown that the frequencies of the two normal modes of the system are

$$\nu_\pm=\left(\tfrac{1}{2}\{[\nu_y^2(1+\mu)+\nu_x^2]\pm\sqrt{[\nu_y^2(1+\mu)+\nu_x^2]^2-4\nu_x^2\nu_y^2}\}\right)^{1/2}\ . \tag{2}$$

A complete description of the system is also given in terms of its normal modes by writing the Hamiltonian as the sum of the Hamiltonians of uncoupled harmonic oscillators having frequencies, equivalent masses, and coordinates of the normal modes, respectively, $\omega_\pm$, $m_\pm$, $\xi_\pm$:

$$H=\frac{p_+^2}{2m_+}+\frac{1}{2}m_+\omega_+^2\xi_+^2+\frac{p_-^2}{2m_-}+\tfrac{1}{2}m_-\omega_-^2\xi_-^2-F_+(t)\xi_+-F_-(t)\xi_-\ . \tag{3}$$

The equivalent masses of the two modes are

$$m_\pm=m_x+\lambda_\pm^2 m_y\ , \tag{4}$$

where the $\lambda_\pm$ parameters are defined as

$$\lambda_\pm=\frac{\nu_y^2}{\nu_y^2-\nu_\pm^2} \tag{5}$$

and the two reduced normal coordinates ξ_- and ξ_+ are

related to x and y by the relations

$$\xi_{\pm}=\frac{\pm(x\lambda_{\mp}-y)}{\lambda_{-}-\lambda_{+}} . \tag{6}$$

$F_{\pm}(t)$ are the components of the applied forces expressed in terms of the normal coordinates and related to f_x and f_y as

$$F_{\pm}(t)=f_x+\lambda_{\pm}f_y . \tag{7}$$

Let us notice that, if the force acting on the transducer is zero ($f_y=0$), we have

$$F_{+}=F_{-}=F(t)=f_x .$$

The variable which is monitored by the transducer is $(y-x)$ Fig. 1, and it can be expressed in terms of normal coordinates:

$$y-x=\xi_{-}(\lambda_{-}-1)+\xi_{+}(\lambda_{+}-1) . \tag{8}$$

III. THE READOUT APPARATUS: THE BACK-ACTION-EVADING PARABRIDGE

We consider the case in which the electromechanical power conversion is obtained by means of a capacitive transducer [2].

In a parametric configuration, the monitored system is dynamically coupled to a readout circuit. This is an electric LC circuit which resonates at the angular frequency $\omega_e \gg \omega_{-},\omega_{+}$. The interaction Hamiltonian between the double harmonic oscillator system and the readout device is

$$\begin{aligned} H_i&=E(t)q(y-x) \\ &=E(t)q[\xi_{-}(\lambda_{-}-1)+\xi_{+}(\lambda_{+}-1)] , \end{aligned} \tag{9}$$

where $E(t)$ is the dynamical electric coupling field (*the pump*). We deal with a continuous monitoring of the harmonic oscillator position, with respect to the case of the stroboscopic measurement approach [9]. In the continuous case, the back-action-evading (BAE) coupling field can be defined, according with [5,6], as

$$\begin{aligned} E(t)=E_{\mathrm{BAE}}(t)&=E_0[\cos\omega_e t\cos(\omega_{+}t)-\cos\omega_e t\cos(\omega_{-}t)] \\ &=\frac{E_0}{2}\{\cos[(\omega_e-\omega_{-})t+\pi]+\cos[(\omega_e+\omega_{-})t+\pi] \\ &\quad+\cos[(\omega_e-\omega_{+})t]+\cos[(\omega_e+\omega_{+})t]\} . \end{aligned} \tag{10}$$

The complete Hamiltonian of the scheme, when a classical force $F(t)$ is applied to the first mechanical oscillator, is

$$\begin{aligned} H=&\frac{p_{+}^2}{2m_{+}}+\frac{1}{2}m_{+}\omega_{+}^2\xi_{+}^2+\frac{p_{-}^2}{2m_{-}}+\frac{1}{2}m_{-}\omega_{-}^2\xi_{-}^2+H_i \\ &+\frac{\phi^2}{2L}+\frac{1}{2}L\omega_e^2q^2-F(t)(\xi_{+}+\xi_{-})-qR(t) . \end{aligned} \tag{11}$$

The quantity q is the charge variation in the capacitive transducer, ϕ is the magnetic flux into the inductor L,

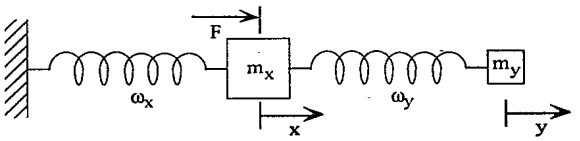

FIG. 1. The mechanical double oscillator system.

and $R(t)$ is the electric noise put in the readout apparatus by the amplifier. Heffner has shown that all linear amplifiers are unavoidably noisy [10]. We schematize the voltage amplifier of the readout circuit following the classic representation given in the literature [11] as it is shown in Fig. 2. The current noise generator acts back, through the circuit, onto the mechanical oscillator. We give later the explicit expression for $R(t)$. Then, six equations can be deduced from the Hamiltonian (11):

$$\begin{aligned} &\dot{p}_{-}=-m_{-}\omega_{-}^2\xi_{-}-E(t)q(\lambda_{-}-1)+F(t) , \\ &\dot{\xi}_{-}=\frac{p_{-}}{m_{-}} , \\ &\dot{p}_{+}=-m_{+}\omega_{+}^2\xi_{+}-E(t)q(\lambda_{+}-1)+F(t) , \\ &\dot{\xi}_{+}=\frac{p_{+}}{m_{+}} , \\ &\dot{\phi}=-L\omega_e^2q+R(t)-E(t)[\xi_{-}(\lambda_{-}-1)+\xi_{+}(\lambda_{+}-1)] , \\ &\dot{q}=\frac{\phi}{L} . \end{aligned} \tag{12}$$

We note that the system (12) describes two normal oscillators, of masses m_{-} and m_{+} and frequencies ν_{-} and ν_{+}, coupled in parallel to the same electric oscillator resonating at ν_e. Two basic requirements characterize a BAE configuration. The former is the particular time-dependent coupling of the parametric readout, expressed by Eq. (10). The latter concerns a proper choice of variables involved by the measurement strategy.

We introduce the components of the complex amplitudes Ξ_{-i}, Ξ_{+i}, and Q_i, where $i=1,2$ of the three oscillators:

$$\begin{aligned} &\Xi_{-2}+j\Xi_{-1}=\frac{1}{\omega_{-}}(\dot{\xi}_{-}+j\omega_{-}\xi_{-})e^{-j\omega_{-}t} , \\ &\Xi_{+2}+j\Xi_{+1}=\frac{1}{\omega_{+}}(\dot{\xi}_{+}+j\omega_{+}\xi_{+})e^{-j\omega_{+}t} , \\ &Q_2+jQ_1=\frac{1}{\omega_e}(\dot{q}+j\omega_e q)e^{-j\omega_e t} . \end{aligned} \tag{13}$$

Substituting these expressions in Eq. (12) we have

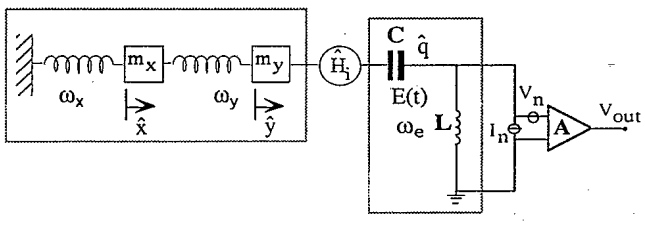

FIG. 2. Complete scheme of the double mechanical oscillator and the readout electric circuit.

$$
\begin{aligned}
\dot{\Xi}_{-1} &= \frac{E(t)(\lambda_- - 1)}{m_-\omega_-}\sin\omega_- t(Q_1\cos\omega_e t + Q_2\sin\omega_e t) - \frac{F(t)}{m_-\omega_-}\sin\omega_- t \ , \\
\dot{\Xi}_{-2} &= -\frac{E(t)(\lambda_- - 1)}{m_-\omega_-}\cos\omega_- t(Q_1\cos\omega_e t + Q_2\sin\omega_e t) + \frac{F(t)}{m_-\omega_-}\cos\omega_- t \ , \\
\dot{\Xi}_{+1} &= \frac{E(t)(\lambda_+ - 1)}{m_+\omega_+}\sin\omega_+ t(Q_1\cos\omega_e t + Q_2\sin\omega_e t) - \frac{F(t)}{m_+\omega_+}\sin\omega_+ t \ , \\
\dot{\Xi}_{+2} &= -\frac{E(t)(\lambda_+ - 1)}{m_+\omega_+}\cos\omega_+ t(Q_1\cos\omega_e t + Q_2\sin\omega_e t) + \frac{F(t)}{m_+\omega_+}\cos\omega_+ t \ , \\
\dot{Q}_1 &= \frac{E(t)}{L\omega_e}\sin\omega_e t(\lambda_- - 1)(\Xi_{-1}\cos\omega_- t + \Xi_{-2}\sin\omega_- t) \\
&\quad + \frac{E(t)}{L\omega_e}\sin\omega_e t(\lambda_+ - 1)(\Xi_{+1}\cos\omega_+ t + \Xi_{+2}\sin\omega_+ t) - \frac{R(t)}{L\omega_e}\sin\omega_e t \ , \\
\dot{Q}_1 &= \frac{E(t)}{L\omega_e}\sin\omega_e t(\lambda_- - 1)(\Xi_{-1}\cos\omega_- t + \Xi_{-2}\sin\omega_- t) \\
&\quad + \frac{E(t)}{L\omega_e}\sin\omega_e t(\lambda_+ - 1)(\Xi_{+1}\cos\omega_+ t + \Xi_{+2}\sin\omega_+ t) - \frac{R(t)}{L\omega_e}\sin\omega_e t \ .
\end{aligned}
\tag{14}
$$

Equations (14) show that the components of complex amplitudes of the oscillators are cross related in couples. If a back action noise $R(t)$ is present in the readout circuit, a monitoring of Q_1 and Q_2, performed to detect an external force $F(t)$, is not effective.

If we introduce the explicit expression of the electric field for the BAE configuration (10) in the system (14), by averaging over periods greater than $2\pi/\omega_+$, $2\pi/\omega_-$, $2\pi/\omega_e$, we have

$$
\begin{aligned}
\dot{\Xi}_{-1} &= -\frac{F(t)}{m_-\omega_-}\sin\omega_- t \ , \\
\dot{\Xi}_{-2} &= +\frac{E_0(\lambda_- - 1)}{4m_-\omega_-}Q_1 + \frac{F(t)}{m_-\omega_-}\cos\omega_- t \ , \\
\dot{\Xi}_{+1} &= -\frac{F(t)}{m_+\omega_+}\sin\omega_+ t \ , \\
\dot{\Xi}_{+2} &= -\frac{E_0(\lambda_+ - 1)}{4m_+\omega_+}Q_1 + \frac{F(t)}{m_+\omega_+}\cos\omega_+ t \ , \\
\dot{Q}_1 &= -\frac{R(t)}{L\omega_e}\sin\omega_e t \ , \\
\dot{Q}_2 &= -\frac{E_0}{4L\omega_e}[\Xi_{-1}(1-\lambda_-) + \Xi_{+1}(\lambda_+ - 1)] \\
&\quad + \frac{R(t)}{L\omega_e}\sin\omega_e t \ .
\end{aligned}
\tag{15}
$$

In Eqs. (15) we synthesize the basic back-action evading (BAE) behavior of the whole system. The components Ξ_{+1} and Ξ_{-1} determine the evolution of Q_2 component of the readout circuit (*forward correlation*). Therefore Q_2 carries information about any interaction of the mechanical oscillator with an external classical force $F(t)$.

The electric noise component $R(t)$ spoils both components of the electric readout, but it is squeezed only onto two homologous mechanical components (*backward correlation*). In such a way the information about $F(t)$ contained in Ξ_{+2} and Ξ_{-2}, which has no forward cross relation, is covered by the noise. A picture of the relations between the six complex amplitude components is shown in Fig. 3.

To improve the sensitivity of actual detectors using the BAE technique two crucial subjects must be taken into account. First, a finite value of the quality factors of the oscillators makes them nonadiabatic and this point is a crucial problem to deal with an experimental setup. The second relevant issue is the presence of the phase and amplitude noise due to the pumps. Present technology allows to obtain high mechanical quality factors by cooling down the mechanical *system* and the readout *apparatus* at low temperatures ($T \leq 100$ mK) [13], although in case of resonant GW antenna (GWA) mechanical quality factors are usually 1 order of magnitude greater than electric ones [12]. Stochastic excitation of the mechanical resonator of the transducer can be avoided by means of a differential capacitor and the electric noise of the pumps is limited by inserting the differential capacitor in a

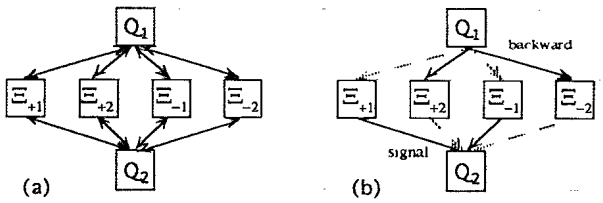

FIG. 3. Picture of relations between the six complex amplitude components. The relations depend on the interaction Hamiltonian: (a) generic; (b) back action evading (BAE).

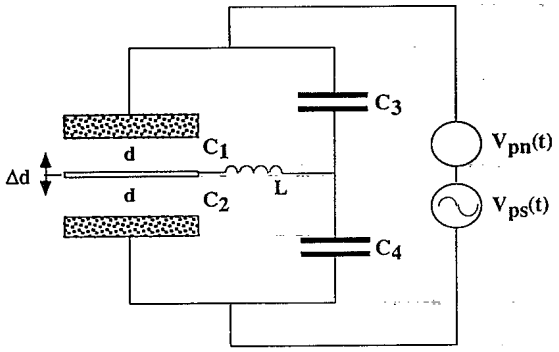

FIG. 4. Parabridge readout configuration.

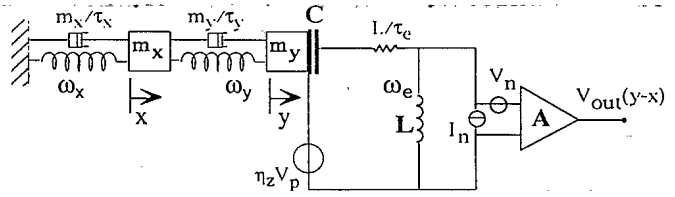

FIG. 5. Picture of the complete scheme taking into account the dissipations. V_p is expressed by (21) in the text.

bridge configuration, as shown in Fig. 4 [8].

The signal pick-up is done at the central arm coil. In this configuration any noise coming from the biasing electric field sources is reduced by the static impedance balance of the bridge η_z that has to be as good as possible.

The equivalent voltage of the central arm is related to the pumps amplitude V_p by the expression

$$V_{\rm eq}=\frac{Z_2Z_3-Z_1Z_4}{(Z_1+Z_2)(Z_3+Z_4)}V_p=\eta_z V_p \ , \tag{16}$$

where

$$Z_n=R_n+\frac{1}{j\omega C_n} \text{ for } n=1,2,3,4 \ . \tag{17}$$

If we suppose to have both a capacitive and resistive unbalance [8], so that $C_1=C_3=C_4=C$, $C_2=C+\Delta C$, $R_1=R_3=R_4=R$, $R_2=R+\Delta R$, with $\omega_e RC\ll 1$, $\Delta R/R<1$, $\Delta C/C\ll 1$, the factor η_z can be written as

$$\eta_z=\frac{1}{4}\omega C\left[\Delta R^2+\left[\frac{\Delta C}{C}\right]^2\frac{1}{\omega^2C^2}\right]^{1/2} . \tag{18}$$

The resistive component of the unbalance is reduced by using superconducting materials and, for the capacitances, low loss dielectric insulators. Hereafter we assume that the unbalance is only due to the capacitive terms.

IV. EQUATIONS OF MOTION OF THE DISSIPATIVE SYSTEM

As discussed in the previous sections the double oscillator system can be completely described in terms of its normal coordinates. In order to analyze the behavior of the actual device the equations of motion must include all dissipative terms. Thus we introduce

$$F_{dm}^{\pm}=-\frac{m_\pm}{\tau_\pm}\dot{\xi}_\pm \ ,$$

where $\tau_\pm$ are the decay times of the normal modes at frequencies $\omega_\pm$, and the electric dissipative term

$$F_{\rm de}=-\frac{L}{\tau_e}\dot{q} \ ,$$

where τ_e is the characteristic decay time of the readout circuit. The term $R(t)$ that appears in the Hamiltonian (11) is expressed as

$$R(t)=L\dot{I}+F_{\rm de} \ ,$$

where I is the back action current due to the amplifier and we include on it also the residual current due to the Johnson noise resistance of the bridge. The output of the physical system shown in Fig. 5 is the voltage at the inductive central arm of the bridge. We will refer all our considerations to this variable instead of the charge variation into the capacitive transducer.

The complete equations in terms of normal coordinates are

$$\ddot{\xi}_-+\frac{1}{\tau_-}\dot{\xi}_-+\omega_-^2\xi_-+\frac{2C}{m_-D}V_pV(\lambda_--1)=\frac{F_-}{m_-} \ ,$$

$$\ddot{\xi}_++\frac{1}{\tau_+}\dot{\xi}_++\omega_+^2\xi_++\frac{2C}{m_+D}V_pV(\lambda_+-1)=\frac{F_+}{m_+} \ ,$$

$$\ddot{V}+\frac{1}{\tau_e}\dot{V}+\omega_e^2V+\frac{\omega_e^2}{2D}V[\xi_+(\lambda_+-1)+\xi_-(\lambda_--1)]=\frac{1}{2C}\dot{I}-\eta_z\omega_e^2V_p \ . \tag{19}$$

Here the coefficients $\lambda_\pm$ come out from the specific interaction Hamiltonian (9) that depends upon the displacement coordinates $(y-x)$ expressed in (8).

To compute the SNR we analyze the response of the apparatus to an impulsive excitation and then we present the noise analysis of the system. To approach this task we express the coordinates involved in (19) by means of their signal (s) and noise (n) components:

$$\xi_+=\xi_{+s}+\xi_{+n} \ , \quad \xi_-=\xi_{-s}+\xi_{-n} \ , \quad V=V_s+V_n \ . \tag{20}$$

Noise sources are basically related to the pumps, to the thermal bath, and to the electronics.

Let us express formally the pump voltage as

$$V_p=V_{ps}+V_{pn} \tag{21}$$

and the external forces as

$$F_\pm(t)=F_s+F_{\pm n} \ , \tag{22}$$

where we assume that the signal (deterministic) is acting onto the bar and $F_{\pm n}$ are the noise components (stochastic) forcing both the mechanical oscillators.

V. RESPONSE OF THE SYSTEM TO AN IMPULSIVE FORCE

If we introduce definitions (20), (21), (22) in (19), separating the signal analysis from the noise one, we obtain, for the former,

$$\ddot{\xi}_{-s}+\frac{1}{\tau_-}\dot{\xi}_{-s}+\omega_-^2\xi_{-s}+\frac{2C}{m_-D}V_{ps}V_s(\lambda_--1)=\frac{F_s(t)}{m_-}\ ,$$

$$\ddot{\xi}_{+s}+\frac{1}{\tau_+}\dot{\xi}_{+s}+\omega_+^2\xi_{+s}+\frac{2C}{m_+D}V_{ps}V_s(\lambda_+-1)=\frac{F_s(t)}{m_+}\ ,$$

$$\ddot{V}_s+\frac{1}{\tau_e}\dot{V}_s+\omega_e^2V_s+\frac{\omega_e^2}{2D}V_{ps}V_s[\xi_{+s}(\lambda_+-1)+\xi_{-s}(\lambda_--1)]=-\eta_z\omega_e^2V_{ps}\ . \quad (23)$$

Then we write the system (23) in terms of the complex amplitudes of the mechanical and electric oscillators Ξ_+, Ξ_-, and V and we specify the pump coupling voltage for the BAE configuration

$$V_{ps}=V_0(\cos\omega_e t\cos\omega_+ t-\cos\omega_e t\cos\omega_- t)\ .$$

We obtain

$$\left[\frac{d}{dt}+\frac{1}{2\tau_\pm}\right]\Xi_{\pm1}=-\frac{F_s}{m_\pm\omega_\pm}\sin\omega_\pm t\ ,$$

$$\left[\frac{d}{dt}+\frac{1}{2\tau_\pm}\right]\Xi_{\pm2}\pm\frac{CV_0}{2m_\pm\omega_\pm D}(\lambda_\pm-1)V_1=\frac{F_s}{m_\pm\omega_\pm}\cos\omega_\pm t\ , \quad (24)$$

$$\left[\frac{d}{dt}+\frac{1}{2\tau_e}\right]V_1=0\ ,$$

$$\left[\frac{d}{dt}+\frac{1}{2\tau_e}\right]V_2+\frac{\beta_e\alpha_{\rm BAE}}{2}[\Xi_{+1}(\lambda_+-1)-\Xi_{-1}(\lambda_--1)]=-\frac{\eta_z\omega_e^2V_0}{2}(\cos\omega_+t-\cos\omega_-t)\ ,$$

with

$$\alpha_{\rm BAE}=\frac{V_0Q_e}{4D}\ .$$

We solve the system in (24) under the hypothesis that the external signal force is a pulse at the time $t=t_0$:

$$F_s(t)=P_0\delta(t-t_0)\ .$$

For $t>t_0$ we obtain the solutions

$$\Xi_{+1}=-\frac{P_0\sin\omega_+t_0}{m_+\omega_+}e^{-(t-t_0)/2\tau_+}\ ,$$

$$\Xi_{+2}=\frac{P_0\cos\omega_+t_0}{m_+\omega_+}e^{-(t-t_0)/2\tau_+}\ ,$$

and

$$\Xi_{-1}=-\frac{P_0\sin\omega_-t_0}{m_-\omega_-}e^{-(t-t_0)/2\tau_-}\ ,$$

$$\Xi_{-2}=\frac{P_0\cos\omega_-t_0}{m_-\omega_-}e^{-(t-t_0)/2\tau_-}\ ,$$

which give, for $\xi_+(t)$ and $\xi_-(t)$,

$$\xi_{+s}(t)=\frac{P_0}{m_+\omega_+}e^{-(t-t_0)/2\tau_+}\sin\omega_+(t-t_0)\ , \quad (25)$$

$$\xi_{-s}(t)=\frac{P_0}{m_-\omega_-}e^{-(t-t_0)/2\tau_-}\sin\omega_-(t-t_0)\ . \quad (26)$$

The vibration amplitude for the transducer with respect to the antenna is

$$y(t)-x(t)=\xi_{+s}(t)(\lambda_+-1)+\xi_{-s}(t)(\lambda_--1)=\frac{P_0(\lambda_+-1)}{m_+\omega_+}e^{-(t-t_0)/2\tau_+}\sin\omega_+(t-t_0)+\frac{P_0(\lambda_--1)}{m_-\omega_-}e^{-(t-t_0)/2\tau_-}\sin\omega_-(t-t_0)\ , \quad (27)$$

where each normal mode responds with an amplitude depending inversely on the corresponding equivalent mass.

We derive the amplitude output voltage from the fifth and sixth equations in (24) obtaining

$$V_1(t)=0\ ,$$

$$V^2(t)=\alpha_{\rm BAE}\frac{P_0(\lambda_+-1)}{m_+\omega_+}\sin\omega_+t_0(e^{-(t-t_0)/2\tau_+}-e^{-(t-t_0)/2\tau_e})-\alpha_{\rm BAE}\frac{P_0(\lambda_--1)}{m_-\omega_-}\sin\omega_-t_0(e^{-(t-t_0)/2\tau_-}-e^{-(t-t_0)/2\tau_e})$$
$$-\eta_z\frac{V_0}{4}\frac{\omega_e}{\omega_+}\left[\sin\omega_+t-\frac{1}{2}\frac{1}{\omega_+\tau_e}\cos\omega_+t\right]+\eta_z\frac{V_0}{4}\frac{\omega_e}{\omega_-}\left[\sin\omega_-t-\frac{1}{2}\frac{1}{\omega_-\tau_e}\cos\omega_-t\right]\ , \quad (28)$$

and

$$V_s(t)=\alpha_{\mathrm{BAE}}\left[\frac{P_0(\lambda_+-1)}{m_+\omega_+}\sin\omega_+t_0(e^{-(t-t_0)/2\tau_+}-e^{-(t-t_0)/2\tau_e})-\frac{P_0(\lambda_--1)}{m_-\omega_-}\sin\omega_-t_0(e^{-(t-t_0)/2\tau_-}-e^{-(t-t_0)/2\tau_e})\right]\sin\omega_e t$$
$$-\eta_z\frac{V_0}{4}\frac{\omega_e}{\omega_+}\left\{\cos(\omega_e-\omega_+)t+\cos(\omega_e+\omega_+)t-\frac{1}{2\omega_+\tau_e}[\sin(\omega_e-\omega_+)t+\sin(\omega_e+\omega_+)t]\right\}$$
$$+\eta_z\frac{V_0}{4}\frac{\omega_e}{\omega_-}\left\{\cos(\omega_e-\omega_-)t+\cos(\omega_e+\omega_-)t-\frac{1}{2\omega_-\tau_e}[\sin(\omega_e-\omega_-)t+\sin(\omega_e+\omega_-)t]\right\}. \quad (29)$$

It is worth noticing that the equations system has been solved by imposing the initial conditions

$$\xi_{+s}(t=0)=0\ ,\quad \xi_{-s}(t=0)=0\ ,$$
$$\dot{\xi}_{+s}(t=0)=0\ ,\quad \dot{\xi}_{-s}(t=0)=0\ ,$$

and by stating that is present a residual current flowing through the central arm, also in absence of a signal, because of the imperfect balance of the bridge:

$$V_s(t=0)=0\ ,\quad \dot{V}_s(t=0)=\eta_z\frac{\omega_e^2V_0}{4\tau_e}\left[\frac{1}{\omega_+^2}-\frac{1}{\omega_-^2}\right].$$

Equation (29) shows that, as in the case of one mechanical oscillator alone, the system is phase sensitive. Furthermore, we have now to consider a more restrictive condition on the electric merit factor,

$$Q_e\gg\frac{\omega_e}{2(\omega_+-\omega_-)}\ ,$$

in order to neglect the Fourier components at frequencies $\omega_e-(\omega_+-\omega_-)$ and $\omega_e+(\omega_+-\omega_-)$. In Fig. 6 the time evolution of the transducer coordinate and the corresponding phase diagrams of the normal coordinates ξ_+ and ξ_- are shown. In Fig. 7 the time evolution of output voltage amplitude and the corresponding phase diagrams of the electrical variable V are shown. We stress that the signal due to the impulsive force is present on phase V_2 alone.

VI. NOISE ANALYSIS

Following the same procedure of the signal analysis we derive the equation describing the noise behavior of the system:

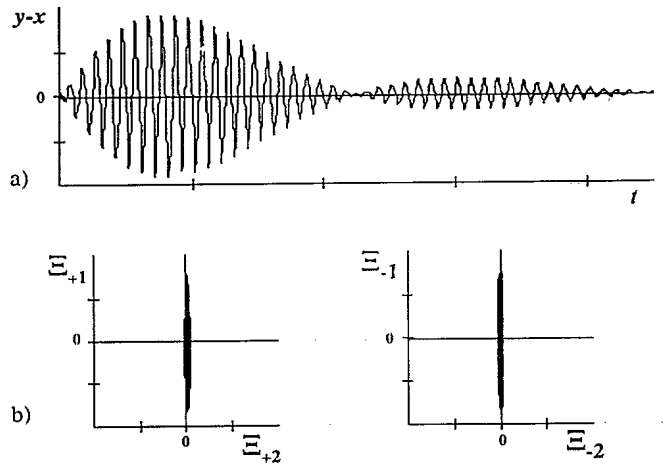

FIG. 6. Theoretical behavior of the transducer: (a) time evolution of the physical displacement coordinate; (b) phase diagrams of the normal coordinates ξ_- and ξ_+.

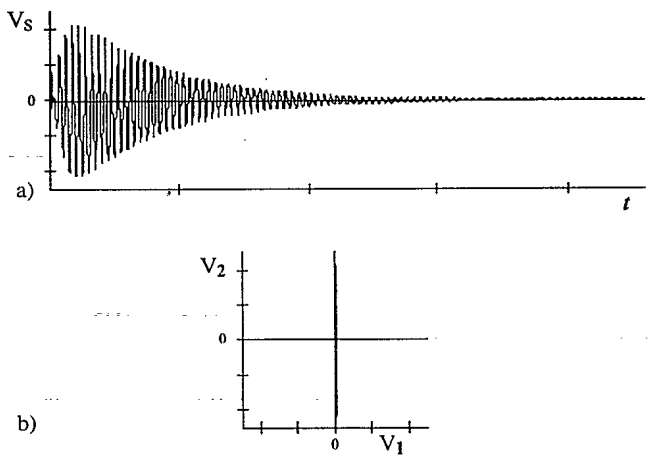

FIG. 7. (a) Time evolution of the response to an impulsive excitation at time $t_0=4\pi/(\omega_++\omega_-)$. (b) Phase diagram of the electrical variable V.

$$\ddot{\xi}_{-n}+\frac{1}{\tau_-}\dot{\xi}_{-n}+\omega_-^2\xi_{-n}+\frac{2CV_pV_n}{m_-D}(\lambda_--1)=\frac{F_n(t)^-}{m_-}-\frac{2C}{m_-D}V_{pn}V_s(\lambda_--1)\,,$$

$$\ddot{\xi}_{+n}+\frac{1}{\tau_+}\dot{\xi}_{+n}+\omega_+^2\xi_{+n}+\frac{2CV_pV_n}{m_+D}(\lambda_+-1)=\frac{F_n(t)^+}{m_+}-\frac{2C}{m_+D}V_{pn}V_s(\lambda_+-1)\,,$$

$$\ddot{V}_n+\frac{1}{\tau_e}\dot{V}_n+\omega_e^2V_n+\frac{\omega_e^2}{2D}V_p[\xi_{+n}(\lambda_+-1)+\xi_{-n}(\lambda_--1)]$$

$$=-\frac{1}{2C}\frac{dI}{dt}-\eta_z\omega_e^2V_{pn}-\frac{\omega_e^2}{2D}V_{pn}[\xi_{+s}(\lambda_+-1)+\xi_{-s}(\lambda_--1)]\,, \tag{30}$$

where $F_n(t)^{\pm}$ are the normal mode forces that take into account the thermal fluctuations of both the mechanical oscillators. In the case of BAE pumping V_{pn} is

$$V_{pn}=\frac{V_0}{2}\{a_1^+\cos(\omega_e+\omega_+)t-\phi_1^+\sin(\omega_e+\omega_+)t-\phi_2^+\sin(\omega_e-\omega_+)t+a_2^+\cos(\omega_e-\omega_+)t\}$$

$$-\frac{V_0}{2}\{a_1^-\cos(\omega_e+\omega_-)t-\phi_1^-\sin(\omega_e+\omega_-)t+a_2^-\cos(\omega_e-\omega_-)t-\phi_2^-\sin(\omega_e-\omega_-)t\}\,. \tag{31}$$

$a_1^{\pm},a_2^{\pm}$ and $\phi_1^{\pm},\phi_2^{\pm}$ are the amplitude and phase fluctuations of the electromagnetic pumps which we assume to have constant uncorrelated power spectra. From Eq. (31) we derive the corresponding linearized equations for the variables Ξ_+, Ξ_-, and V:

$$\left[\frac{d}{dt}+\frac{1}{2\tau_\pm}\right]\Xi_{\pm1}=n_{\pm1}(\lambda_\pm-1)\,,$$

$$\left[\frac{d}{dt}+\frac{1}{2\tau_\pm}\right]\Xi_{\pm2}\pm\left[\frac{CV_0}{2m_\pm\omega_\pm D}\right]V_1(\lambda_\pm-1)$$

$$=n_{\pm2}(\lambda_\pm-1)\,,$$

$$\left[\frac{d}{dt}+\frac{1}{2\tau_e}\right]V_1=n_3\,, \tag{32}$$

$$\left[\frac{d}{dt}+\frac{1}{2\tau_e}\right]V_2+\frac{\beta_e\alpha_{\rm BAE}}{2}[\Xi_{+1}(\lambda_+-1)$$

$$-\Xi_{-1}(\lambda_--1)]=n_4\,,$$

where $n_{\pm i}$, $i=1,2$, n_3,n_4 include the thermal forces and noise terms due to the pumps and the amplifier. In the Appendix the full expressions of these terms are given. All the other terms depend upon the product of the output variables times the noise fluctuation of the pumps. We consider these terms as perturbations in the case of small signals.

In the n_3 and n_4 terms we consider, in the first approximation, only contributes depending upon the current noise of the output amplifier and the terms due to the bias voltage V_{pn}. To obtain the output noise spectra we solve Eqs. (32) in the frequency domain by introducing for each stochastic variable the corresponding bilateral noise power spectrum. For a complete presentation of the algebra procedure we refer to [14]. We recall here our fundamental assumptions: (1) The readout circuit is able to filter out the $2\omega_e$, $2\omega_\pm$ terms and the higher harmonics; (2) all the source of noise are uncorrelated; (3) the power spectra of the fluctuations of the electromagnetic pumps are constant: i.e.,

$$S_{a_1^\pm}=S_{a_2^\pm}=S_a,\quad S_{\phi_1^\pm}=S_{\phi_2^\pm}=S_\phi\,.$$

The power spectrum of the quantities

$$-\frac{F_n(t)}{m_\pm\omega_\pm(\lambda_\pm-1)}\sin\omega_\pm t\,,$$

$$\frac{F_n(t)}{m_\pm\omega_\pm(\lambda_\pm-1)}\cos\omega_\pm t\,,$$

in both cases is equal to

$$\frac{\beta_\pm}{(\lambda_\pm-1)^2}\frac{k_bT}{m_\pm\omega_\pm^2}\,.$$

Following a perturbation approach we obtain the first order spectra

$$S^0_{n_{\pm_1}}=S^0_{n_{\pm_2}}=S^\pm_{nb}=\frac{1}{m_\pm\omega_\pm^2}\left[\frac{\beta_\pm k_bT}{(\lambda_\pm-1)^2}+\eta_z^2\beta^\pm_{\rm BAE}C\left[\frac{\omega_e}{Q_e}\right]^2\left\{\left[\frac{V_0}{2}\right]^2\left[S_a+S_\phi\left[\frac{\beta_e}{2\omega_\pm}\right]^2\right]+\left[S_a+S_\phi\left[\frac{\beta_e}{2\omega_\mp}\right]^2\right]\right\}\right]\,, \tag{33}$$

$$S_{n_3^0}=S_{n_4^0}=S_{w\bar{b}}=\frac{1}{8C^2}\left[S_{I_n}+\frac{2k_bT}{R}\right]+(\eta_z\omega_e)^2\frac{V_0^2}{2}(S_a+S_\phi)\,, \tag{34}$$

where

$$\beta_{\mathrm{BAE}}^{\pm}=\frac{C\alpha_{\mathrm{BAE}}^2}{m_{\pm}\omega_{\pm}^2}$$

are the energy coupling factors between the mechanical normal modes $\omega_{\pm}$ and the electric oscillator.

Finally we obtain the spectral densities of the output voltage components:

$$S_{V_1}=\frac{\frac{1}{2}\left[S_{I_n}\left[\frac{Q_e}{\omega_e C}\right]^2+2k_bT\left[\frac{Q_e}{\omega_e C}\right]\right]+(\eta_z Q_e)^2\frac{V_0^2}{2}(S_a+S_\phi)}{\left[1+\left[2Q_e\frac{\omega}{\omega_e}\right]^2\right]}+S_{V_n}, \tag{35}$$

$$S_{V_2}=S_{V_1}+\frac{\frac{\alpha_{\mathrm{BAE}}^2(\lambda_+-1)^2}{m_+\omega_+^2}\left[k_bT+\eta_z^2\beta_{\mathrm{BAE}}^{+}\frac{Q_+}{Q_e}\omega_e C(S_{V_{np}^+}+S_{nc}^+)\right]}{\frac{1}{4}\frac{\omega_+}{Q_+}\left[1+\left[2Q_e\frac{\omega}{\omega_e}\right]^2\right]\left[1+\left[2Q_+\frac{\omega}{\omega_+}\right]^2\right]}$$

$$+\frac{\frac{\alpha_{\mathrm{BAE}}^2(\lambda_--1)^2}{m_-\omega_-^2}\left[k_bT+\eta_z^2\beta_{\mathrm{BAE}}^{-}\frac{Q_-}{Q_e}\omega_e C(S_{V_{np}^-}+S_{nc}^-)\right]}{\frac{1}{4}\frac{\omega_-}{Q_-}\left[1+\left[2Q_e\frac{\omega}{\omega_e}\right]^2\right]\left[1+\left[2Q_-\frac{\omega}{\omega_-}\right]^2\right]}, \tag{36}$$

where

$$S_{V_{np}^{\pm}}=\left[\frac{V_0}{2}\right]^2\frac{\omega_e}{\omega_\pm Q_e}\left[S_a+S_\phi\left[\frac{\omega_e}{2\omega_\pm Q_e}\right]^2\right] \tag{37}$$

and

$$S_{nc}^{\pm}=\left[\frac{V_0}{2}\right]^2\frac{\omega_e}{\omega_\pm Q_e}\left[S_a+S_\phi\left[\frac{\omega_e}{2\omega_\mp Q_e}\right]^2\right]\left[\frac{\omega_\pm}{\omega_\mp}\right]^2. \tag{38}$$

The quantity (37) represents the perturbation effect of the bias pumps at the frequencies $(\omega_e-\omega_+)$, $(\omega_e+\omega_+)$ on the normal mode ω_+ (a similar effect is present for the ω_- mode and the other two pumps), while the quantity (38) represents a crossed effect of the pumps $(\omega_e-\omega_+)$, $(\omega_e+\omega_+)$ on the normal mode ω_- (a similar effect is present for the other pumps and the mode ω_+).

We note from (35) and (36) that the noise behavior of the two-oscillators system is very similar to the single-oscillator one. On S_{V_1} the wideband noise contribution terms are only present whereas on S_{V_2} there are also in addition two narrow-band terms. These are composed by the contributions of the signal due to the Brownian motion and the residual noise terms due to the electromagnetic pumps that depends on η_z.

Then, in spite of the larger complexity of this scheme, we obtain the same results derived for the single oscillator [8]. If the balance of the bridge makes negligible the noise of the electromagnetic pumps the narrow-band noise terms are only due to the Brownian motion of the mechanical oscillators and the system is back action evading [16].

VII. SIGNAL-TO-NOISE RATIO

We have shown in the previous sections that the response of the system to a mechanical excitation is contained in one (e.g., V_2) component of the complex electric output signal. Moreover, the peculiarity of this phase sensitivity is that two noise terms are present, both having the spectrum bandwidths of the mechanical resonances ω_- and ω_+. These two terms, due to the thermal noise plus the residual pump noise, are referred to the normal modes of the system.

As is usually done in the sensitivity analysis of a gravitational wave detector an equivalent equipartition temperature of the system can be defined that, in this case, is related to only one phase of the transducer output:

$$T_{\mathrm{eq}}=\frac{V_{nb}^2}{\alpha_{\mathrm{BAE}}^2k_b\left[\frac{(\lambda_+-1)^2}{m_+\omega_+^2}+\frac{(\lambda_--1)^2}{m_-\omega_-^2}\right]}$$

$$=T\left\{1+\eta_z^2\left[\frac{\omega_eL}{Q_e}\right]\frac{1}{k_bT\left[\frac{(\lambda_+-1)^2}{m_+\omega_+^2}+\frac{(\lambda_--1)^2}{m_-\omega_-^2}\right]}\sum_{i=+,-}Q_i\beta_{\mathrm{BAE}}^{i}\frac{(\lambda_i-1)^4}{m_i\omega_i^2}(S_{V_{np}}^{(i)}+S_{nc}^{(i)})\right\}, \tag{39}$$

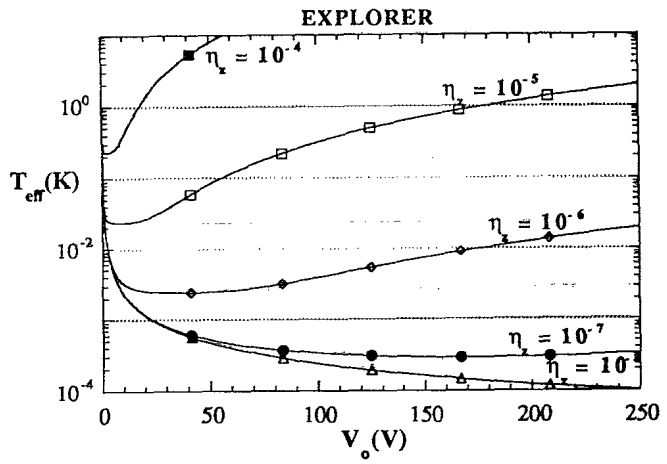

FIG. 8. $T_{\rm eff}$ vs V_0 using the balance factor η_z as a parameter: performance of Explorer GWA.

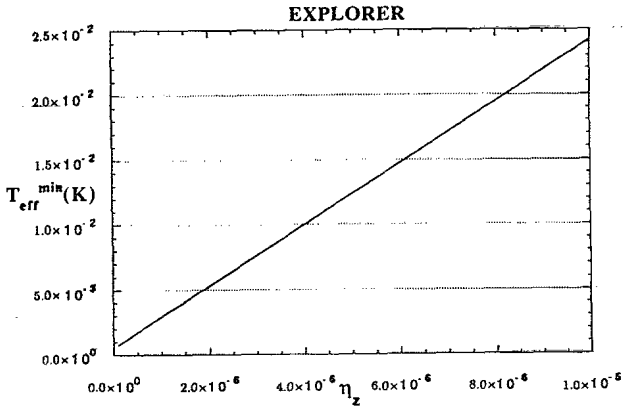

FIG. 10. Best sensitivity of Explorer GWA versus balance parameter η_z.

where V_{nb}^2 is the variance of the narrow band noise measured at the transducer output. $T_{\rm eq}$ can be regarded as a measure of the energy sensitivity of the detector. From (39) it follows that if the second term is made negligible with respect to 1, either lowering the pump noise or obtaining a low value for η_z, there is no back action of the amplifier on the mechanical oscillator. For the detection of burst signals the energy variation sensitivity is more significant. The usual way to evaluate this sensitivity in resonant bar detector experiments is to introduce an effective temperature of the detector $T_{\rm eff}$. In this case $T_{\rm eff}$ will be obtained by optimizing the signal to noise ratio S/N on the sensitive phase of the detector. Following the general theory of data analysis [18], the general expression for the signal to noise ratio verifies the inequality

$$\left[\frac{S}{N}\right]^2=\frac{|V_{2_s}(t_0)|^2}{E(|V_{2_n}(t_0)|^2)}$$

$$\leq\frac{1}{2\pi}\int_{-\infty}^{+\infty}\frac{|H(\omega)|^2}{SV_2(\omega)}d\omega\,, \tag{40}$$

where $H(\omega)$ represents the transfer function of the optimum filter that we are trying to derive. In order to introduce the effective temperature we assume that S/N is equal to 1 and the response of the system for an impulsive signal is maximized. The release of energy in the antenna is given by

$$k_b T_{\rm eff}=\frac{P_0^2}{2m_x}\,. \tag{41}$$

The compact expression for the effective temperature is obtained:

$$T_{\rm eff}=\frac{\pi}{4m_x k_b}\left[\int_{-\infty}^{+\infty}\frac{\mathcal{A}+\mathcal{B}\omega^2}{a+b\omega^2+c\omega^4+d\omega^6}d\omega\right]^{-1}$$

$$=\frac{\pi}{4m_x k_b}\frac{1}{I}\,, \tag{42}$$

where

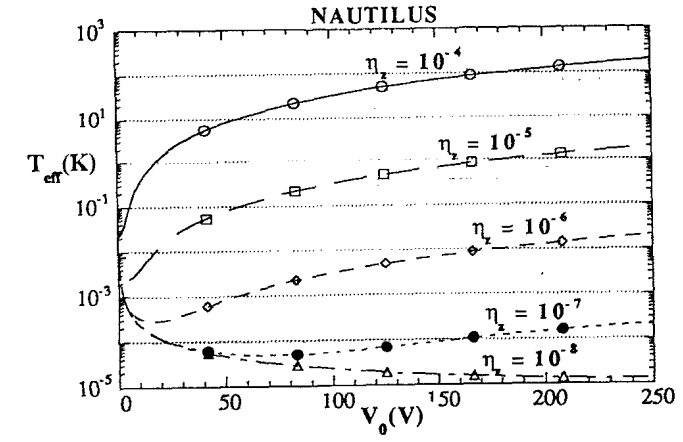

FIG. 9. $T_{\rm eff}$ vs V_0 using the balance factor η_z as a parameter: performance of Nautilus GWA.

TABLE I. Mechanical parameters of cryogenic GWA's Explorer and Nautilus.

	Explorer	Nautilus
T	2 K	100 mK
m_x	1135 kg	1160 kg
ν_x	915 Hz	915 Hz
$Q_+ = Q_-$	1×10^6	5×10^6

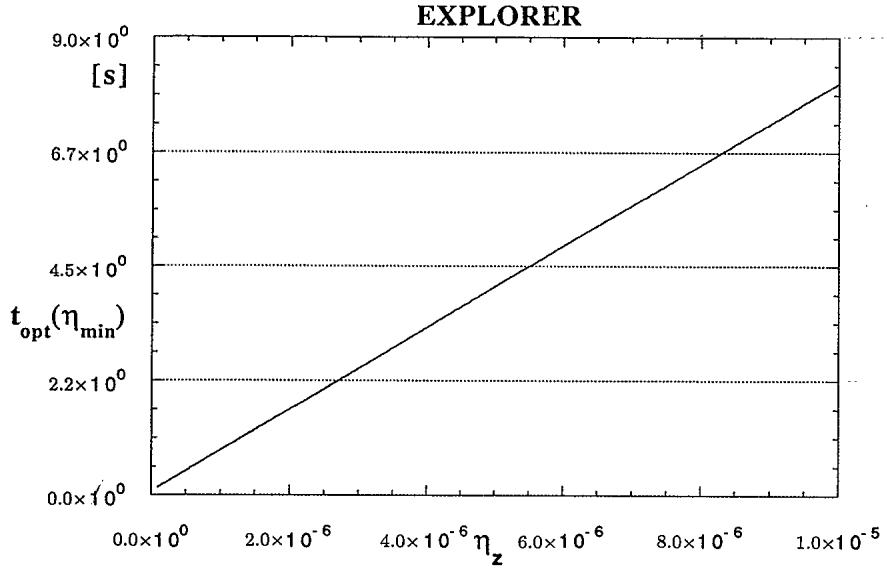

FIG. 11. Optimum time corresponding to the best sensitivity versus the balance parameter in the case of Explorer GWA.

$$
\begin{aligned}
a &= S_{uu}^{+} + S_{uu}^{-} + S_{ee} + S_{V_n} , \\
b &= S_{uu}^{-} \left[\frac{2Q_+}{\omega_+} \right]^2 + S_{uu}^{+} \left[\frac{2Q_-}{\omega_-} \right]^2 + (S_{ee} + S_{V_n}) \left[\left[\frac{2Q_-}{\omega_-} \right]^2 + \left[\frac{2Q_+}{\omega_+} \right]^2 \right] + S_{V_n} \left[\frac{2Q_e}{\omega_e} \right]^2 , \\
c &= S_{ee} \left[\frac{2Q_+}{\omega_+} \frac{2Q_-}{\omega_-} \right]^2 + S_{V_n} \left[\left[\frac{2Q_+}{\omega_+} \frac{2Q_-}{\omega_-} \right]^2 + \left[\frac{2Q_+}{\omega_+} \frac{2Q_e}{\omega_e} \right]^2 + \left[\frac{2Q_e}{\omega_e} \frac{2Q_-}{\omega_-} \right]^2 \right] , \\
d &= S_{V_n} \left[\frac{2Q_+}{\omega_+} \frac{2Q_-}{\omega_-} \frac{2Q_e}{\omega_e} \right]^2 , \\
\mathcal{A} &= \alpha_{\mathrm{BAE}}^2 \left[\frac{Q_+}{\omega_+} \frac{\sin\omega_+ t_0(\lambda_+ - 1)}{m_+ \omega_+} - \frac{Q_-}{\omega_-} \frac{\sin\omega_- t_0(\lambda_- - 1)}{m_- \omega_-} \right]^2 , \\
\mathcal{B} &= \left[\frac{2Q_+ Q_-}{\omega_+ \omega_-} \right]^2 \alpha_{\mathrm{BAE}}^2 \left[\frac{\sin\omega_+ t_0(\lambda_+ - 1)}{m_+ \omega_+} - \frac{\sin\omega_- t_0(\lambda_- - 1)}{m_- \omega_-} \right]^2 ,
\end{aligned}
\tag{43}
$$

in which we have set

$$
S_{ee} = \frac{1}{2} \left[S_{I_n} \left[\frac{Q_e}{\omega_e C} \right]^2 + 2k_b T \left[\frac{Q_e}{\omega_e C} \right] \right] + (\eta_z Q_e)^2 \left[\frac{V_0^2}{2} \right] (S_a + S_\phi) \tag{44}
$$

and

$$
S_{uu}^{\pm} = \frac{4Q_\pm}{\omega_\pm} \frac{\alpha_{\mathrm{BAE}}^2 (\lambda_\pm - 1)^2}{m_\pm \omega_\pm^2} \left[k_b T + \eta_z^2 \beta_{\mathrm{BAE}}^{\pm} \frac{Q_\pm}{Q_e} \omega_e C (S_{V_{np}}^{\pm} + S_{V_{nc}}^{\pm}) \right] . \tag{45}
$$

The equivalent bandwidth W of the detector can also be computed as

$$
W = \frac{\int_{-\infty}^{\infty} y_f(\omega) d\omega}{y_f(\omega = 0)} = \frac{I}{G_s(0)} = I \frac{a}{\mathcal{A}} , \tag{46}
$$

where $G_s(0)$ is the function spectral gain and $y_f(\omega)$ is the Fourier transform of the system response at the output of the optimum filter.

W corresponds to the inverse of the optimum integration time:

$$
t_{\mathrm{opt}} = \frac{2\pi}{W} . \tag{47}
$$

TABLE II. Typical parameters of BAE scheme.

$S_{I_n} = 5 \times 10^{-28}\ A^2/\mathrm{Hz}$	$S_{V_n} = 1.8 \times 10^{-19}\ V^2/\mathrm{Hz}$
$S_\phi = -135$ dBc/Hz	$T_n = 6.9 \times 10^{-1}$ K
$\nu_e = 200\,000$ Hz	$Q_e = 10\,000$

VIII. DISCUSSION AND CONCLUSIONS

The detection sensitivity depends on several parameters of the system as it has shown by the expressions

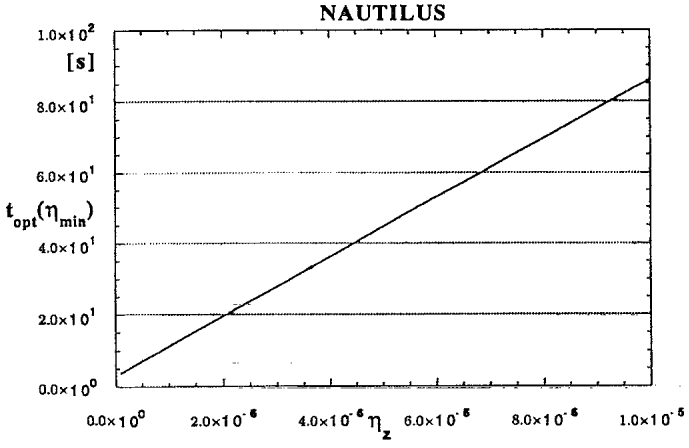

FIG. 12. Optimum time corresponding to the best sensitivity versus the balance parameter in the case of Nautilus GWA.

given in the previous section. The optimization of the effective temperature $T_{\rm eff}$ and the optimum detection time $t_{\rm opt}$ can be performed by studying these dependences in a specific case. We consider the typical features of cryogenic GWA's [12,13] under development (Table I) and combining the parameters of these double mechanical oscillators with those of different BAE setups. In Figs. 8 and 9 the prediction of the sensitivity versus the coupling voltage is shown for various values of the balance η_z. These trends are derived by assuming for the parameters S_{I_n}, S_{V_n}, S_ϕ, Q_e, and ν_e those reported in Table II. All these values are realistic at the present status of technology and the corresponding transducer systems can be assembled using commercial instruments. We stress that best performances are obtained when the balance factor is low and the coupling voltage amplitude is high. The $T_{\rm eff}$ has a minimum whose value depends on the η_z parameter. In Fig. 10 the plot of the minimum values of $T_{\rm eff}$ is shown to be linearly dependent on η_z. In Figs. 11 and 12 the optimum times are plotted versus the balance parameter η_z. In Tables III and IV we synthesize our results for different hypotheses about the pump noise level.

The best sensitivity is reached by using very low noise pumps and low values of balance factor. Oscillators with a phase noise of the order of -165 dBc are commercially available [17].

We observe that a BAE configuration could be also applied successfully to cryogenic GWA's cooled at 2 K, improving remarkably their sensitivity. With these detectors, usually operated in a linear detection scheme, a typical figure sensitivity of 5 mK is reached. Moreover this scheme would play a crucial role for ultra GWA's, allowing them to reach the planned figure of ($T \simeq 10^{-7}$ K) near the quantum limit of this detector, well below the best sensitivity achievable in a linear configuration (0.1 mK) [18].

ACKNOWLEDGMENTS

We wish to thank Dr. R. Onofrio and Dr. M. Bassan for the critical reading of the manuscript and for the helpful discussions.

APPENDIX

In this appendix we report the complete expressions of the noise terms appearing in the system (32):

$$
\begin{aligned}
n_{\pm 1} = & -\frac{F_n(t)^{\pm}}{\omega_{\pm} m_{\pm}(\lambda_{\pm}-1)}\sin\omega_{\pm}t + \frac{2CV_{pn}V_s}{\omega_{\pm}m_{\pm}D}\sin\omega_{\pm}t \pm \left[\frac{CV_0}{4m_{\pm}\omega_{\pm}D}\right][V_1(\phi_2^{\pm}-\phi_1^{\pm})+V_2(a_1^{\pm}-a_2^{\pm})] \\
& \mp \left[\frac{CV_0}{2m_{\pm}\omega_{\pm}D}\right]\{\cos\omega_{\mp}t\,\sin\omega_{\pm}t[-V_2(\phi_1^{\mp}+\phi_2^{\mp})+V_1(a_1^{\mp}+a_2^{\mp})] \\
& + \sin\omega_{\pm}t\,\sin\omega_{\mp}t[V_2(a_2^{\mp}+a_1^{\mp})+V_1(\phi_2^{\mp}-\phi_1^{\mp})]\}\,, \qquad \text{(A1)} \\
n_{\pm 2} = & \frac{F_n(t)^{\pm}}{\omega_{\pm} m_{\pm}(\lambda_{\pm}-1)}\cos\omega_{\pm}t - \frac{2CV_{pn}V_s}{\omega_{\pm}m_{\pm}D}\sin\omega_{\pm}t \mp \left[\frac{CV_0}{4m_{\pm}\omega_{\pm}D}\right][-V_2(\phi_2^{\pm}+\phi_1^{\pm})+V_1(a_1^{\pm}+a_2^{\pm})] \\
& \pm \left[\frac{CV_0}{2m_{\pm}\omega_{\pm}D}\right]\{\cos\omega_{\mp}t\,\cos\omega_{\pm}t[-V_2(\phi_1^{\mp}+\phi_2^{\mp})+V_1(a_1^{\mp}+a_2^{\mp})]
\end{aligned}
$$

TABLE III. Best sensitivity and corresponding optimum time for GWA Explorer considering different pump noise levels.

	−123 dBc/Hz			−135 dBc/Hz			−165 dBc/Hz		
η_z	V_0	$T_{\rm eff}^{\rm min}$	$t_{\rm opt}$	V_0	$T_{\rm eff}^{\rm min}$	$t_{\rm opt}$	V_0	$T_{\rm eff}^{\rm min}$	$t_{\rm opt}$
10^{-4}	0.7 V	0.96 K	317 s	1.9 V	0.21 K	72.9 s	16.9 V	7.4 mK	2.5 s
10^{-5}	3.1 V	94 mK	32.7 s	8.5 V	21 mK	7.35 s	79.3 V	810 μK	0.26 s
10^{-6}	14.5 V	9.6 mK	3.3 s	45.7 V	2.2 mK	0.72 s	347 V	120 μK	25 ms
10^{-7}	65.5 V	1 mK	0.33 s	175.3 V	270 μK	81 ms	1227 V	31 μK	7.7 ms

TABLE IV. Best sensitivity and corresponding optimum time for GWA Nautilus considering different pump noise levels.

	−123 dBc/Hz			−135 dBc/Hz			−165 dBc/Hz		
η_z	V_0	$T_{\rm eff}^{\rm min}$	$t_{\rm opt}$	V_0	$T_{\rm eff}^{\rm min}$	$t_{\rm opt}$	V_0	$T_{\rm eff}^{\rm min}$	$t_{\rm opt}$
10^{-4}	0.1 V	0.2 K	3882.2 s	0.6 V	34 mK	803 s	7.9 V	810 μK	26.3 s
10^{-5}	1.1 V	14 mK	463.42 s	3.6 V	2.4 mK	81.1 s	36.7 V	110 μK	2.9 s
10^{-6}	6.1 V	1.4 mK	45.5 s	16.6 V	290 μK	8.71 s	138.6 V	24 μK	0.5 s
10^{-7}	23.6 V	180 μK	5.2 s	70.6 V	48 μK	1 s	450 V	7 μK	0.1 s

$$+\cos\omega_{\pm}t\,\sin\omega_{\mp}t[V_2(a_2^{\mp}+a_1^{\mp})+V_1(\phi_2^{\mp}-\phi_1^{\mp})]\}\ , \tag{A2}$$

$$\begin{aligned} n_3=&\left[\frac{\dot I}{2\omega_e C}+\eta_z\omega_e V_{pn}\right]\sin\omega_e t+\frac{\omega_e}{2D}V_{pn}[\xi_{+s}(\lambda_+-1)+\xi_{-s}(\lambda_--1)]\sin\omega_e t\\ &+\frac{\beta_e\alpha_{\rm BAE}}{4}\{[\Xi_{+2}(a_2^+-a_1^+)-\Xi_{+1}(\phi_2^++\phi_1^+)](\lambda_+-1)-[\Xi_{-2}(a_2^--a_1^-)-\Xi_{-1}(\phi_2^-+\phi_1^-)](\lambda_--1)\}\\ &+\frac{\beta_e\alpha_{\rm BAE}}{2}\{-[\Xi_{+1}[(a_2^--a_1^-)\cos\omega_+t\,\sin\omega_-t-(\phi_2^-+\phi_1^-)\cos\omega_+t\,\cos\omega_-t]\\ &\quad+[\Xi_{+2}[(a_2^--a_1^-)\sin\omega_+t\,\sin\omega_-t-(\phi_2^-+\phi_1^-)\sin\omega_+t\,\cos\omega_-t]](\lambda_+-1)\\ &\quad+[\Xi_{-1}[(a_2^+-a_1^+)\cos\omega_-t\,\sin\omega_+t-(\phi_2^++\phi_1^+)\cos\omega_-t\,\cos\omega_+t]\\ &\quad+[\Xi_{-2}[(a_2^+-a_1^+)\sin\omega_-t\,\sin\omega_+t-(\phi_1^++\phi_2^+)\sin\omega_-t\,\cos\omega_+t]](\lambda_--1)\}\ , \end{aligned} \tag{A3}$$

$$\begin{aligned} n_4=&-\left[\frac{\dot I}{2\omega_e C}+\eta_z\omega_e V_{pn}\right]\cos\omega_e t-\frac{\omega_e}{2D}V_{pn}[\xi_{+s}(\lambda_+-1)+\xi_{-s}(\lambda_--1)]\cos\omega_e t\\ &+\frac{\beta_e\alpha_{\rm BAE}}{4}\{[\Xi_{+2}(\phi_2^+-\phi_1^+)-\Xi_{+1}(a_2^+-a_1^+)](\lambda_+-1)-[\Xi_{-2}(\phi_2^--\phi_1^-)-\Xi_{-1}(a_2^--a_1^-)](\lambda_--1)\}\\ &+\frac{\beta_e\alpha_{\rm BAE}}{2}\{-[\Xi_{+1}[(a_2^-+a_1^-)\cos\omega_+t\,\cos\omega_-t+(\phi_2^--\phi_1^-)\cos\omega_+t\,\sin\omega_-t]\\ &\quad+[\Xi_{+2}[(a_2^-+a_1^-)\sin\omega_+t\,\cos\omega_-t+(\phi_2^--\phi_1^-)\sin\omega_+t\,\sin\omega_-t]](\lambda_+-1)\\ &\quad+[\Xi_{-1}[(a_2^++a_1^+)\cos\omega_-t\,\cos\omega_+t-(\phi_2^+-\phi_1^+)\cos\omega_-t\,\sin\omega_+t]\\ &\quad+[\Xi_{-2}[(a_2^++a_1^+)\cos\omega_-t\,\cos\omega_+t+(\phi_2^+-\phi_1^+)\sin\omega_+t\,\cos\omega_-t]](\lambda_--1)\}\ . \end{aligned} \tag{A4}$$

[1] H. J. Paik, in Proceedings of 55th International School of Physics Enrico Fermi, Varenna (1972).
[2] P. Rapagnani, Nuovo Cimento C **5**, 385 (1982).
[3] R. Giffard, Phys. Rev. D **14**, 2478 (1976).
[4] V. B. Braginsky and F. Y. Khalili, *Quantum Measurements,* edited by K. S. Thorne (Cambridge University Press, Cambridge, England, 1991).
[5] C. M. Caves, K. S. Thorne, R. W. P. Drever, V. D. Sandberg, and M. Zimmerman, Rev. Mod. Phys. **52**, 341 (1980).
[6] M. F. Bocko, L. Narici, D. H. Douglass, and W. W. Johnson, Phys. Lett. **97A**, 259 (1983).
[7] O. D. Augiar, W. W. Johnson, and W. O. Hamilton, Rev. Sci. Instrum. **62**, 2523 (1991).
[8] C. Cinquegrana, E. Majorana, P. Rapagnani, and F. Ricci, Phys. Rev. D **48**, 2478 (1993).
[9] R. Onofrio and A. Rioli, Phys. Rev. D **47**, 2176 (1993).
[10] H. Heffner, Proc. I.R.E. **50**, 1604 (1962).
[11] C. D. Motchenbacher and F. C. Fitchen, *Low-Noise Electronic Design* (Wiley, New York, 1973).
[12] P. Astone, M. Bassan, P. Bonifazi, P. Carelli, M. G. Castellano, G. Cavallari, E. Coccia, C. Cosmelli, V. Fafone, S. Frasca, E. Majorana, I. Modena, G. V. Pallottino, G. Pizzella, P. Rapagnani, F. Ricci, and M. Visco, Phys. Rev. D **47**, 362 (1993).
[13] P. Astone, M. Bassan, P. Bonifazi, P. Carelli, M. G. Castellano, G. Cavallari, E. Coccia, C. Cosmelli, V. Fafone, S. Frasca, E. Majorana, I. Modena, G. V. Pallottino, G. Pizzella, P. Rapagnani, F. Ricci, and M. Visco, Europhys. Lett. **16**, 231 (1991).
[14] P. Puppo, Laurea thesis (unpublished), Università di Roma "La Sapienza" (1993).
[15] A. Papoulis, *Probability, Random Variables and Stochastic Processes* (McGraw-Hill, New York, 1991).
[16] E. Majorana, N. Pergola, P. Puppo, R. Rapagnani, and F. Ricci, Phys. Lett. A **180**, 43 (1993).
[17] FCXO stabilized quartz oscillator by Oscilloquartz of Neuchâtel, Switzerland.
[18] N. Solomonson, W. O. Hamilton, and W. Johnson, Rev. Sci. Instum. **65**, 1 (1994).